

Autoactivation of Mouse Trypsinogens Is Regulated by Chymotrypsin C via Cleavage of the Autolysis Loop^{*}

Received for publication, April 18, 2013, and in revised form, June 3, 2013. Published, JBC Papers in Press, June 28, 2013, DOI 10.1074/jbc.M113.478800

Balázs Csaba Németh[‡], Thomas Wartmann[§], Walter Halangk[§], and Miklós Sahin-Tóth^{‡1}

From the [‡]Department of Molecular and Cell Biology, Boston University Henry M. Goldman School of Dental Medicine, Boston, Massachusetts 02118 and the [§]Division of Experimental Surgery, Department of Surgery, Otto-von-Guericke-Universität Magdeburg, D-39120 Magdeburg, Germany

Background: Hereditary pancreatitis-associated mutations alter regulation of trypsinogen activation by chymotrypsin C.

Results: Activation of mouse trypsinogens T8 and T9 is inhibited by chymotrypsin C-mediated cleavage of the autolysis loop.

Conclusion: Chymotrypsin C regulates activation of human and mouse trypsinogens by different mechanisms.

Significance: Introduction of human pancreatitis-associated mutations into mouse trypsinogens will not recapitulate the pathogenic biochemical effects.

Chymotrypsin C (CTRC) is a proteolytic regulator of trypsinogen autoactivation in humans. CTRC cleavage of the trypsinogen activation peptide stimulates autoactivation, whereas cleavage of the calcium binding loop promotes trypsinogen degradation. Trypsinogen mutations that alter these regulatory cleavages lead to increased intrapancreatic trypsinogen activation and cause hereditary pancreatitis. The aim of this study was to characterize the regulation of autoactivation of mouse trypsinogens by mouse Ctrc. We found that the mouse pancreas expresses four trypsinogen isoforms to high levels, T7, T8, T9, and T20. Only the T7 activation peptide was cleaved by mouse Ctrc, causing negligible stimulation of autoactivation. Surprisingly, mouse Ctrc poorly cleaved the calcium binding loop in all mouse trypsinogens. In contrast, mouse Ctrc readily cleaved the Phe-150–Gly-151 peptide bond in the autolysis loop of T8 and T9 and inhibited autoactivation. Mouse chymotrypsin B also cleaved the same peptide bond but was 7-fold slower. T7 was less sensitive to chymotryptic regulation, which involved slow cleavage of the Leu-149–Ser-150 peptide bond in the autolysis loop. Modeling indicated steric proximity of the autolysis loop and the activation peptide in trypsinogen, suggesting the cleaved autolysis loop may directly interfere with activation. We conclude that autoactivation of mouse trypsinogens is under the control of mouse Ctrc with some notable differences from the human situation. Thus, cleavage of the trypsinogen activation peptide or the calcium binding loop by Ctrc is unimportant. Instead, inhibition of autoactivation via cleavage of the autolysis loop is the dominant mechanism that can mitigate intrapancreatic trypsinogen activation.

Hereditary chronic pancreatitis is a human genetic disorder caused by heterozygous mutations in the serine protease 1

^{*} This work was supported, in whole or in part, by National Institutes of Health Grants R01DK058088, R01DK082412, R01DK082412-S2, and R01DK095753 (to M. S.-T.). This work was also supported by Grant DFG HA2080/7-1 from the Deutsche Forschungsgemeinschaft.

¹ To whom correspondence should be addressed: 72 East Concord St., Evans-433, Boston, MA 02118. Tel.: 617-414-1070; Fax: 617-414-1041; E-mail: miklos@bu.edu.

(*PRSS1*) gene, which codes for the digestive proenzyme cationic trypsinogen (1). High penetrance trypsinogen mutations such as p.N29I and p.R122H are associated with an autosomal dominant inheritance pattern, whereas mutations with lower penetrance, exemplified by p.A16V, may be found not only in hereditary but also in sporadic cases with no family history (2). The disease mechanism involves increased autoactivation of mutant trypsinogens within the pancreas due to altered regulation by chymotrypsin C (CTRC)² (3). Autoactivation of human trypsinogens is proteolytically regulated by CTRC that cleaves cationic trypsinogen at two distinct regulatory sites. Cleavage of the Phe-18–Asp-19 peptide bond in the activation peptide results in a shorter activation peptide and increased autoactivation (4). This cleavage is stimulated by pancreatitis-associated mutations p.N29I and p.A16V (3, 4). Cleavage of the Leu-81–Glu-82 peptide bond in the calcium binding loop, together with the trypsin-mediated autolytic cleavage of the Arg-122–Val-123 peptide bond, results in rapid degradation and inactivation of cationic trypsinogen (5). Mutations p.N29I and p.R122H hamper CTRC-mediated degradation and thereby increase trypsinogen autoactivation (3).

Despite the significant progress in understanding the mechanism of trypsinogen mutations at the biochemical level, animal models that recapitulate the human disease both phenotypically and mechanistically remain unavailable. Transgenic mice carrying the coding DNA for human cationic trypsinogen with the p.R122H mutation did not develop spontaneous pancreatitis, although small differences in the pathological responses were noted when pancreatitis was artificially induced (6). In contrast, when mice were made transgenic with the p.R122H mutation introduced into mouse trypsinogen isoform T8 (see Table 1), the resulting animals developed acute and eventually chronic pancreatitis (7). Unfortunately, this remarkable model has never been made available to the pancreas research community for independent replication nor have there been any follow-up studies published by the original authors since 2006. It thus remains unclear whether the

² The abbreviations used are: CTRC, chymotrypsin C; IPG, immobilized pH gradient.

TABLE 1

Trypsinogen genes in the mouse genome

Table is based on the 1997 GenBank™ submissions AE000663.1, AE000664.1, and AE000665.1, which first reported the genomic sequence of the mouse T cell receptor β locus. The original annotation described genes T2 and T14 as relic genes based on the absence of exon 1. The more recent annotation to the mouse genome identified the first exons for both genes, and we re-classified these as pseudogenes.

Gene	Function	Notes
T1	Pseudogene	Exons give in-frame translation; product may serve unknown function
T2	Pseudogene	Also known as protease, serine 58 (Prss58), GenBank™ NM_175020.3
T3	Pseudogene	Exons give in-frame translation; product may serve unknown function
T4	Functional	A single nucleotide deletion in exon 2 leads to a frameshift
T5	Functional	
T6	Relic	This gene has only exons 2 and 3
T7	Functional	
T8	Functional	Also known as trypsin4 (Try 4), GenBank™ NM_011646.5
T9	Functional	Also known as trypsin5 (Try 5) GenBank™ NM_001003405.4 Also known as TESP4, GenBank™ AB017031.1
T10	Functional	
T11	Functional	Also known as protease, serine,3 (Prss3), GenBank™ NM_011645.2
T12	Functional	
T13	Relic	This gene has only exons 3 and 5
T14	Pseudogene	This gene has a defective splice site after exon 2
T15	Functional	
T16	Functional	Also known as protease, serine,1 (Prss1), GenBank™ NM_053243.2
T17	Relic	This gene is missing exons 1 and 2
T18	Relic	This gene is missing exons 1 and 2
T19	Relic	This gene has only exon 3
T20	Functional	Also known as protease, serine,2 (Prss2), GenBank™ NM_009430.2

observed phenotype was related to the expression of the mutant trypsinogen. Nonetheless, this study raises the question whether the biochemical effects of the p.R122H mutation are similar in the context of mouse and human trypsinogens and whether we can utilize mouse trypsinogens to model the human condition.

Considering the widespread use of mice in experimental studies of the pancreas, it is surprising how little is known about mouse trypsinogens. Watanabe and Ogasawara (8) reported the purification of three trypsinogen isoforms from the mouse pancreas. Stevenson *et al.* (9) cloned a trypsinogen cDNA, corresponding to isoform T20, from the pancreas and demonstrated that the mouse genome contained multiple different trypsinogen genes. This was later confirmed by Hood and co-workers in 1997 (10) who sequenced the mouse T cell receptor β locus on chromosome 6 and identified 20 trypsinogen genes organized in two groups, one containing genes T1–T7 and the other containing genes T8–T20 (Table 1). Eleven of the 20 genes are potentially functional (Table 1 and Fig. 1), whereas the other nine genes are pseudogenes or relic genes. Ohmura *et al.* (11) cloned the cDNA for isoform T9 from sperm acrosome. It remains unknown, however, which isoforms of the 11 potentially functional trypsinogen genes are expressed at the protein level in the mouse pancreas. More recently, genetic deletion of T7 indicated that this isoform may contribute as much as 60% of pancreatic trypsinogens (12, 13). The authors also found that despite the presence of other trypsinogen isoforms, mice deficient in T7 did not respond to secretagogue hyperstimulation with the characteristic intra-acinar cell trypsinogen activation, an early event in acute pancreatitis. These new findings suggest that the different mouse trypsinogen isoforms vary in their activation kinetics and highlight the need for their comparative biochemical characterization. Therefore, in this study, we identified the major trypsinogen isoforms in the mouse pancreas, expressed these recombinantly, and studied their autoactivation and regulation by mouse Ctrc.

EXPERIMENTAL PROCEDURES

Nomenclature—Amino acid residues are numbered starting with the initiator methionine of the primary translation product, according to the recommendations of the Human Genome Variation Society. Note that because of an extra Asp residue (Asp-23) in the activation peptide of T7, amino acid numbering in this isoform is shifted by one relative to human and other mouse trypsinogens. Autolysis loop refers to the flexible region between residues 146 and 154 in trypsinogen (Fig. 1).

Plasmid Construction and Mutagenesis—Construction of the pTrapT7-intein-Hu1 and pcDNA3.1(–)-CTRB2 expression plasmids harboring the coding sequence for human cationic trypsinogen (Hu1) and human chymotrypsinogen B2 (CTRB2) was reported previously (5, 14). Mutation p.S150F was introduced into human cationic trypsinogen using overlap-extension PCR mutagenesis. Expression plasmids for mouse trypsinogens were created in the pTrapT7 plasmid previously designed for bacterial expression of human trypsinogens (15, 16). The coding DNA was PCR-amplified from commercial IMAGE clones and cloned into pTrapT7 using NcoI and Sall restriction sites. In all constructs, the N-terminal secretory signal peptide was replaced with a Met-Ala sequence. In T20, the stop codon was changed from amber (TAG) to ochre (TAA). T7 was amplified from IMAGE clone 30306963 (GenBank™ accession BC061093.1) using T7 NcoI sense (5'-AAA TTT CCA TGG CTC TCC CCC TGG ATG ATG ATG ATG-3', where the NcoI site is underlined) and T7 Sall antisense (5'-AAA TTT GTC GAC TTA GTT GGC AGC GAT GGT CTG CTG-3', where the Sall site is underlined) primers. T8 was amplified from IMAGE clone 30306436 (GenBank™ accession BC061135.1) using T8 NcoI sense (5'-AAA TTT CCA TGG CTT TCC CTG TGG ATG ATG ATG ACA-3', where the NcoI site is underlined) and T8 Sall antisense (5'-AAA TTT GTC GAC TTA GTT TGC AGC AAT GGT GTT TTG-3', where the

Sall site is underlined) primers. T9 was amplified from IMAGE clone 6433372 (GenBankTM accession CF581321.1) using T8 NcoI sense and T9 Sall antisense (5'-AAA TTT GTC GAC TTA GTT TGC GGC AAT GGT GTC CTG-3', where the Sall site is underlined) primers. T20 was amplified from IMAGE clone 6433384 (GenBankTM accession CF581305.1) using T20 NcoI sense (5'-AAA TTT CCA TGG CTT TCC CTG TGG ATG ATG ATG ACA-3', where the NcoI site is underlined) and T20 Sall antisense (5'-AAA TTT GTC GAC TTA GTT GTC AGC AAT TGT GTT CTG-3', where the Sall site is underlined) primers. Mutations p.L82A, p.R123H, and p.L149A in T7 and p.R122H in T8 were created by overlap extension PCR and cloned into the pTrapT7 plasmid.

Expression plasmids for mouse chymotrypsinogens carrying a His₁₀ affinity tag were created in the pcDNA3.1(-) plasmid. The coding DNA for mouse chymotrypsinogen C (Ctrc) was PCR-amplified from a cDNA preparation from CD-1 mouse pancreas, using mouse CTRC XhoI sense (5'-AAA TTT CTC GAG ACC TGA ACC ATG TTG GGA ATT ACA GTC-3', where the XhoI site is underlined) and mouse CTRC EcoRI antisense (5'-AAA TTT GAA TTC GGC GTC GAG ACT TCT GGA ACC GTC TCT-3', where the EcoRI site is underlined) primers and cloned into pcDNA3.1(-) using XhoI and EcoRI. A His₁₀ affinity tag was added to the C terminus using gene synthesis (GenScript, Piscataway, NJ) and the XcmI and EcoRI sites. In this synthetic construct Leu-268 was deleted to prevent autolytic cleavage of the His tag. The coding DNA for mouse chymotrypsinogen B (Ctrb, GenBankTM accession NM_025583.2) with a C-terminal His₁₀ tag was custom-synthesized (GenScript) and cloned into pcDNA3.1(-) using XhoI and BamHI.

Purification and Identification of Trypsinogens from CD-1 Mouse Pancreas—Pancreata (2 to 3) were homogenized in 10 ml of 20 mM Na-HEPES (pH 7.4) buffer, briefly sonicated, and centrifuged at 13,500 rpm for 10 min, and ~4 ml of supernatant was loaded onto a 2-ml ecotin column. Ecotin is a pan-serine protease inhibitor from *Escherichia coli*, which can bind the inactive zymogen forms of pancreatic serine proteases (17, 18). The ecotin column was washed with 20 mM Tris-HCl (pH 8.0), 0.2 M NaCl, and trypsinogens were eluted with 50 mM HCl. The flow-through contained no trypsinogen, as judged by the lack of trypsin activity after incubation with enteropeptidase. The ecotin-eluate contained all trypsinogen isoforms and low levels of chymotrypsinogen and proelastase. Four ml of eluate was loaded onto a 2-ml Mono S column equilibrated with 20 mM sodium acetate (pH 5.0), and trypsinogens were eluted with a 0–0.5 M NaCl gradient at 1 ml/min flow rate (Fig. 2A). The eluted proteins were separated by SDS-PAGE and transferred to a PVDF membrane, and individual bands were subjected to N-terminal protein sequencing by Edman degradation (Midwest Analytical, St. Louis, MO). Peaks corresponding to T8, T9, and T20 were also subjected to in-gel digestion followed by LC-MS/MS mass spectrometry (ProtTech, Phoenixville, PA). Relative abundance of trypsinogen isoforms was calculated from the peak areas corrected for the ultraviolet extinction coefficient differences. The T9-T8 peaks were also corrected for Ctrb contamination, which was determined from the relative trypsin

and chymotrypsin activities after activation with enteropeptidase. Because of the poor separation of T8 and T9, these two isoforms were calculated as one.

Identification of Trypsinogens from NMRI Mouse Pancreas by Two-dimensional PAGE and Mass Spectrometry—Pancreata were homogenized in a Potter homogenizer at 2,500 rpm in ice-cold homogenization buffer (HS buffer, 250 mM sucrose, 10 mM citric acid (pH 6.0), 0.5 mM EGTA, 0.1 mM MgSO₄) with Complete mini protease inhibitor mixture (Roche Applied Science). The homogenate was centrifuged for 5 min at 500 × g, and the post-nuclear supernatant was centrifuged at 1,300 × g for 15 min at 4 °C. This zymogen granule-enriched pellet was washed with HS buffer and dissolved in sample buffer (5 M urea, 2 M thiourea, 2 M CHAPS, 2% ASB-14, 0.05% SB3–10) with Complete mini protease inhibitor mixture and stored in aliquots at –80 °C.

Immobilized pH gradient (IPG) strips (pH 3–10, 13 cm) were rehydrated overnight in sample buffer containing 65 mM (10 mg/ml) dithiothreitol (DTT), 2% IPG buffer, and 0.01% Serva blue. The zymogen granule-enriched pancreatic extract dissolved in sample buffer (50–100 μg) was supplemented with 65 mM (10 mg/ml) DTT, 2% IPG buffer, 0.01% Serva blue and cup-loaded at the anode end of the strips. Isoelectric focusing was performed under mineral oil at 3,500 V with a current limit of 50 μA per strip up to 8,000 total volt hours using an IPGphor unit (Amersham Biosciences). Strips were subsequently incubated in equilibration buffer (0.5 M Tris-HCl (pH 8.8), 6 M urea, 2% SDS, 30% glycerol) containing 50 mM DTT followed by incubation in 0.3 M acrylamide, for 15 min each. For electrophoresis in the second dimension, the IPG strips were applied onto a 10.5% SDS-polyacrylamide gel, and proteins were separated according to Schaeffer and van Jagow (19). Gels were stained with silver nitrate by a modified method of Blum *et al.* (20). For estimation of relative protein content of trypsinogen spots, gels were further stained with Serva blue, according to Neuhoff *et al.* (21). Gel images were analyzed, and spot intensities were quantitated with the ImageMaster 2D Elute version 3.10 software (Amersham Biosciences). Protein spots of interest were excised, de-stained, and digested in-gel with sequencing grade bovine trypsin (Roche Applied Science, 12.5 ng/μl) overnight at 37 °C. Peptides were extracted from gel slices, and mass spectra were analyzed using MALDI-TOF Reflex III mass spectrometer machine (Bruker Daltonics, Germany) in linear mode with external calibration. Peptide fingerprint data analysis was performed using the web-based ProFound database with a mass tolerance of 250 ppm.

Expression and Purification of Trypsinogens—Human cationic trypsinogen was expressed in the aminopeptidase P-deficient LG-3 *E. coli* strain as fusions with a self-splicing mini-intein, as described previously (14, 22). Mouse trypsinogens were expressed in *E. coli* BL21(DE3), as described for human trypsinogens previously (15, 16). Isolation of cytoplasmic inclusion bodies, *in vitro* refolding, and purification with ecotin affinity chromatography were performed according to published protocols (14–16, 18, 22). The preparations were more than 90% pure, as judged by SDS-PAGE and Coomassie Blue staining. Concentrations of trypsinogen solutions were calculated from their UV absorbance at 280 nm

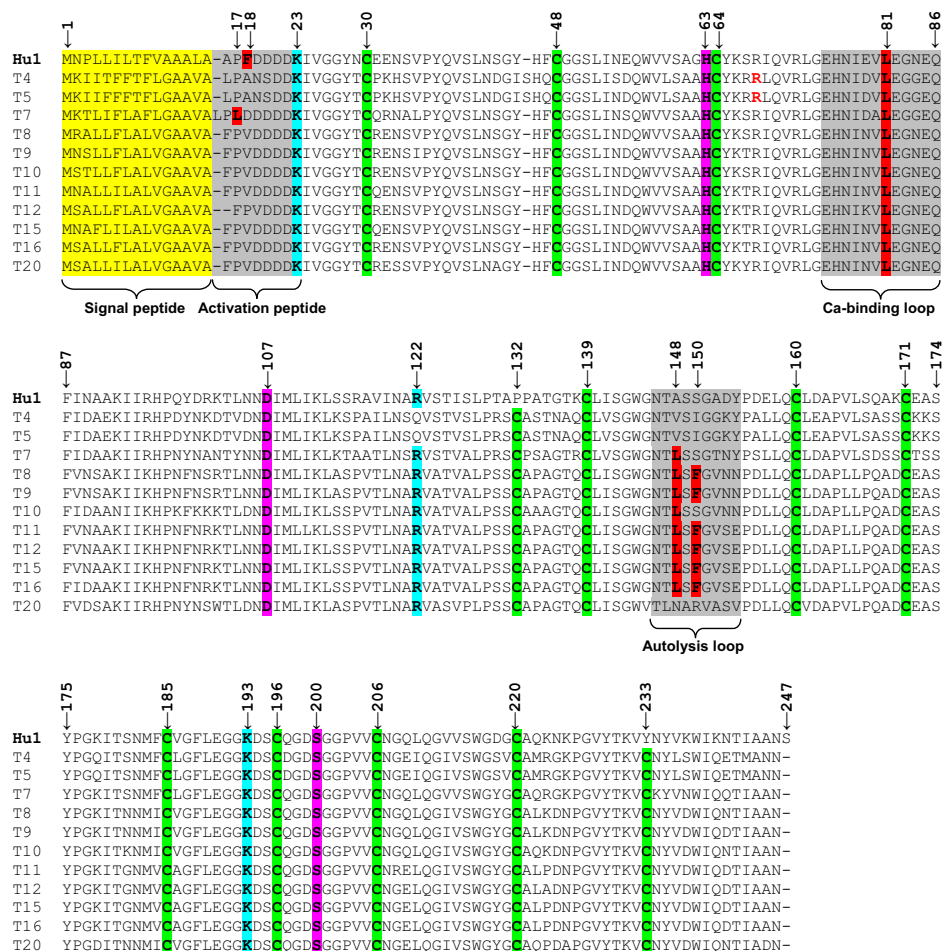


FIGURE 1. Primary sequence alignment of human cationic trypsinogen (Hu1) and 11 potentially functional mouse trypsinogens. Numbering starts with the initiator methionine. Note that due to insertions in T4, T5, and T7, the numbering is shifted by one after the insertion sites, relative to the indicated numbers. Similarly, a deletion in T12 shifts numbering. Trypsin cleavage sites are highlighted in blue and chymotrypsin C cleavage sites in red. Cys residues are indicated in green and the catalytic triad in magenta. The original annotation predicted deletion of Arg-69 (red letter) in T4 and T5, but more recent annotations include this residue. See text for details.

using the following extinction coefficients: $37,525 \text{ M}^{-1}\text{cm}^{-1}$ (human cationic trypsinogen), $39,140 \text{ M}^{-1}\text{cm}^{-1}$ (mouse T7), $34,670 \text{ M}^{-1}\text{cm}^{-1}$ (mouse T8 and T9), and $43,150 \text{ M}^{-1}\text{cm}^{-1}$ (mouse T20).

Expression and Purification of Chymotrypsinogens—Human CTRB2 and mouse Ctrb and Ctrc carrying His₁₀ affinity tags were expressed in transiently transfected HEK 293T cells and purified from 450 ml of conditioned medium using nickel affinity chromatography as reported previously (3, 23). Aliquots (75 μl) of the eluted 5-ml fractions were analyzed by 15% SDS-PAGE and Coomassie Blue staining, and peak fractions with >90% purity were pooled and dialyzed for 72 h against three changes of 1 liter of 0.1 M Tris-HCl (pH 8.0) buffer containing 150 mM NaCl. The dialyzed chymotrypsinogen solutions were concentrated using a Vivaspin 20 concentrator (10-kDa molecular mass cutoff). Chymotrypsinogens were activated with trypsin, and active chymotrypsin concentrations were determined by active site titration with ecotin, as described previously (24).

Trypsinogen Autoactivation—Trypsinogen at 2 μM concentration was incubated in the absence or presence of 25 nM chymotrypsin, as indicated, and 10 nM initial trypsin in 0.1 M Tris-

HCl (pH 8.0), 1 or 10 mM CaCl₂, and 0.05% Tween 20 (final concentrations) at 37 °C. At given times, 1.5- μl aliquots were withdrawn and mixed with 48.5 μl of assay buffer containing 0.1 M Tris-HCl (pH 8.0), 1 mM CaCl₂, and 0.05% Tween 20. Trypsin activity was measured by adding 150 μl of 200 μM N-CBZ-Gly-Pro-Arg-*p*-nitroanilide substrate dissolved in assay buffer and following the release of the yellow *p*-nitroaniline at 405 nm in a SpectraMax plus384 microplate reader (Molecular Devices, Sunnyvale, CA) for 1 min. Reaction rates were calculated from fits to the initial linear portions of the curves.

Trypsinogen Activation with Enteropeptidase—To determine the maximal trypsin activity attainable after full activation, 2 μM trypsinogen was incubated in 0.1 M Tris-HCl (pH 8.0), 10 mM CaCl₂, and 0.05% Tween 20 (final concentrations) at 37 °C with 140 ng/ml final concentration of human enteropeptidase (R&D Systems, Minneapolis, MN) for 1 h, and trypsin activity was measured as described above. This activity was designated as 100%, and trypsin activity measured in autoactivation experiments was expressed relative to this value. The 100% values corresponded to 500 (T7), 400 (T8), 400 (T9), and 300 (T20) milli-OD/min readings.

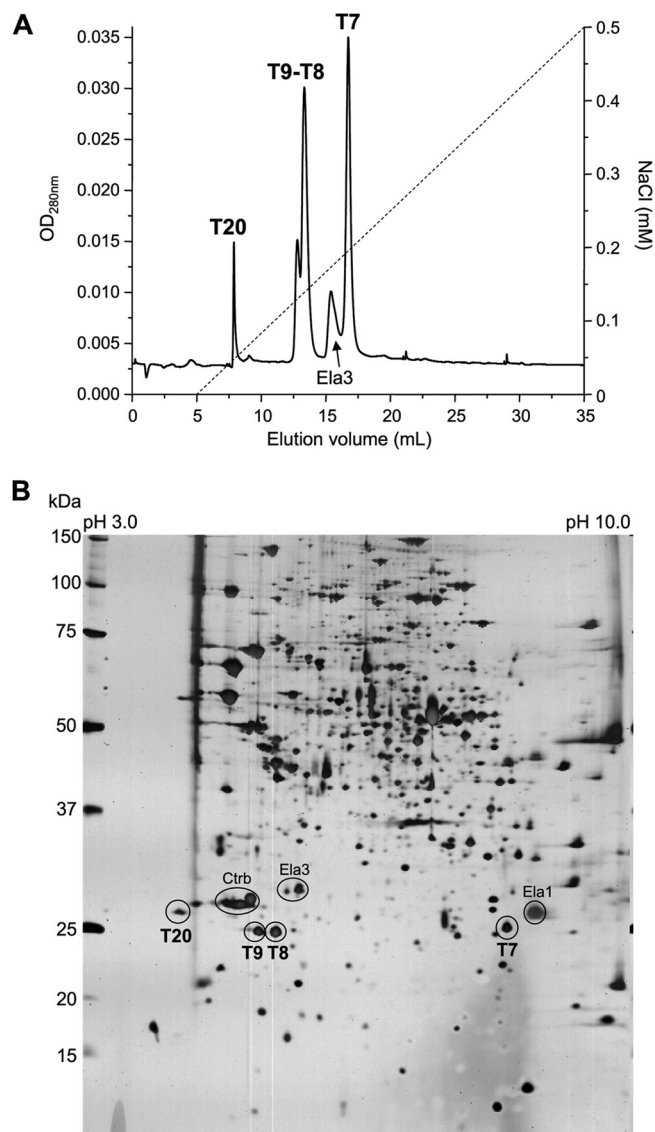


FIGURE 2. Identification of major trypsinogen isoforms expressed in the mouse pancreas. *A*, chromatographic separation of trypsinogen isoforms. Trypsinogens were purified from pancreas tissue extracts of CD-1 mice using ecotin affinity chromatography, and the ecotin eluate was loaded onto a Mono S column equilibrated with 20 mM sodium acetate (pH 5.0). The column was developed with a linear gradient of 0–0.5 M NaCl. Peaks were analyzed by SDS-PAGE, N-terminal sequencing, and mass spectrometry, as described under “Experimental Procedures” and “Results.” *B*, two-dimensional PAGE of a zymogen granule-enriched fraction of pancreas tissue from NMRI mice. Silver-stained spots were digested with trypsin and analyzed by peptide mass fingerprinting, as described under “Experimental Procedures.” Spots for trypsinogen isoforms T7, T8, T9, and T20, proelastase 3 (Ela3); chymotrypsinogen B (Ctrb), and proelastase 1 (Ela1) are indicated.

Gel Electrophoresis—Trypsinogen samples (75 μ l, \sim 3.8 μ g of protein) were precipitated with trichloroacetic acid (10% final concentration), and the precipitate was recovered by centrifugation, dissolved in 15 μ l of Laemmli sample buffer containing 100 mM DTT (final concentration), and heat-denatured at 95 $^{\circ}$ C for 5 min. Electrophoretic separation was performed on 15% SDS-PAGE mini gels in standard Tris-glycine buffer. Gels were stained with Brilliant Blue R-250 and destained as described earlier (25). Quantitation of bands was carried out with the GelDoc XR+ gel documentation system and Image Lab 3.0 software (Bio-Rad).

TABLE 2

Relative expression levels of major trypsinogen isoforms in the mouse pancreas determined by ion exchange chromatography (CD-1) or two-dimensional gel electrophoresis (NMRI)

The averages from four experiments \pm S.D. are indicated. See text for details.

Mouse strain	Relative expression levels (% of total)			
	T7	T8	T9	T20
CD-1	41 \pm 1	47 \pm 3		12 \pm 2
NMRI	25 \pm 1	33 \pm 1	27 \pm 1	15 \pm 2

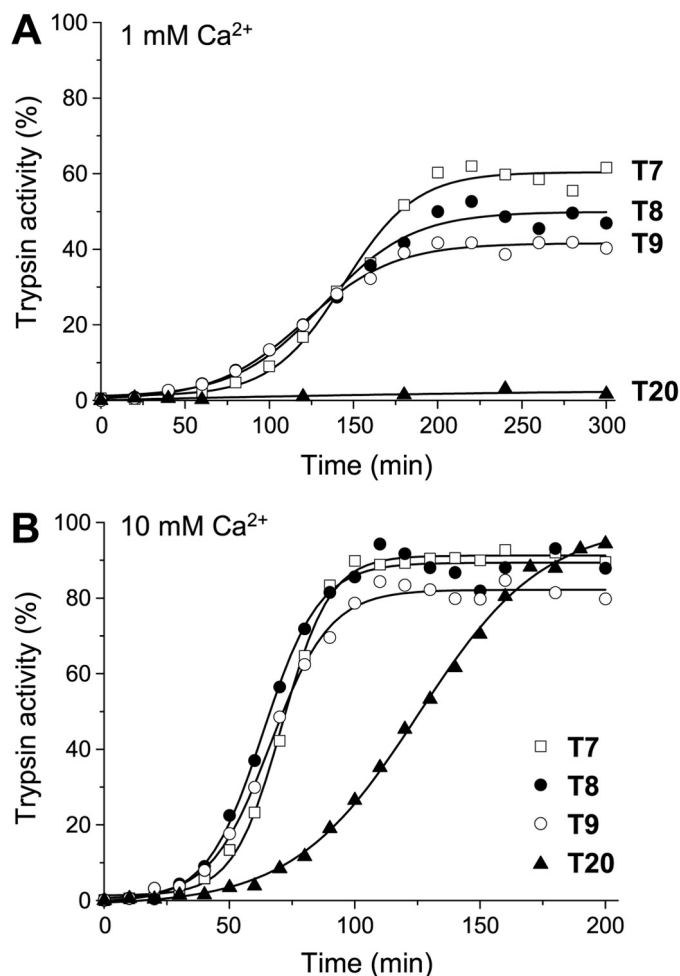


FIGURE 3. Autoactivation of mouse trypsinogens. Trypsinogens were incubated at 2 μ M concentration with 10 nM initial trypsin in 0.1 M Tris-HCl (pH 8.0), 1 mM CaCl₂ (*A*) or 10 mM CaCl₂ (*B*) and 0.05% Tween 20 at 37 $^{\circ}$ C. Aliquots (1.5 μ l) were withdrawn at the indicated times, and trypsin activity was determined as described under “Experimental Procedures.” Trypsin activity was expressed as percentage of the maximal activity determined by full activation with enteropeptidase. Representative experiments from four replicates are shown.

RESULTS

Identification of Major Trypsinogen Isoforms in the Mouse Pancreas—To identify trypsinogen isoforms expressed at high levels in the mouse pancreas, we used ecotin-affinity chromatography to purify trypsinogens *en bloc* from pancreas tissue extracts of the outbred CD-1 mouse strain. Trypsinogens were eluted under acidic conditions from the ecotin column and immediately loaded onto a Mono S cation exchange column equilibrated with 20 mM sodium acetate (pH 5.0). The Mono S column was developed with a NaCl gradient, resulting in five

Mouse Trypsinogens

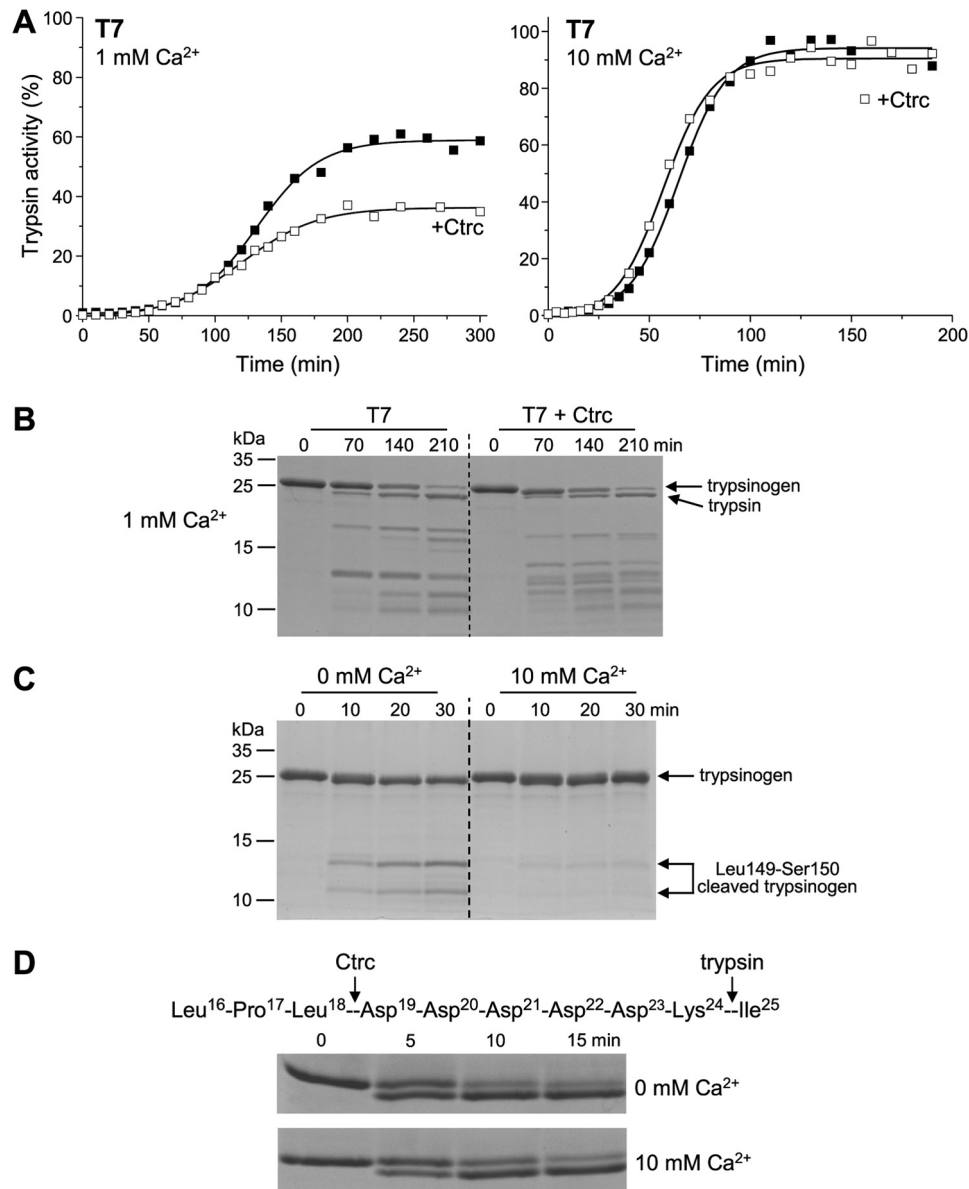


FIGURE 4. Effect of mouse Ctrc on mouse trypsinogen T7. *A*, autoactivation was measured in 1 and 10 mM CaCl₂ in the absence (*solid symbols*) or presence (*open symbols*) of 25 nM mouse Ctrc, as described under "Experimental Procedures." *B*, SDS-PAGE analysis of the autoactivation reaction in 1 mM CaCl₂. Samples were withdrawn at the indicated time points, precipitated with trichloroacetic acid, electrophoresed, and stained as described under "Experimental Procedures." *C*, cleavage of T7 trypsinogen by 25 nM mouse Ctrc. Incubations were performed with 2 μM trypsinogen in 0.1 M Tris-HCl (pH 8.0) in the absence or presence of 10 mM CaCl₂. Samples were precipitated with trichloroacetic acid and analyzed by SDS-PAGE and Coomassie Blue staining. Representative experiments from three replicates are shown. *D*, cleavage of the activation peptide of trypsinogen T7 by mouse Ctrc. Primary structure of the native T7 activation peptide with proteolytic cleavage sites for Ctrc and trypsin is also indicated. Note that the N-terminal amino acid of mature trypsinogen is Leu-16, as the 15-amino acid-long secretory signal peptide is removed in the endoplasmic reticulum. Trypsinogen was incubated at 2 μM concentration with 25 nM Ctrc in 0.1 M Tris-HCl (pH 8.0) and 0 or 10 mM CaCl₂ (final concentrations) at 37 °C. To prevent autoactivation, 25 nM human SPINK1 trypsin inhibitor was included. At the indicated times, reactions were terminated by precipitation with trichloroacetic acid, and samples were analyzed by nonreducing SDS-PAGE and Coomassie Blue staining. Relevant segments of representative gels (from two replicates) demonstrate the small mobility shift of the trypsinogen band caused by Ctrc-mediated cleavage of the Leu-18–Asp-19 peptide bond. Note that the rapid rate of cleavage is partly due to the added Met-Ala sequence at the N terminus of recombinant T7.

peaks (Fig. 2A). Edman degradation unambiguously identified the small fourth peak as proelastase 3 (N terminus is CGQPS) and the large fifth peak as the cationic T7 trypsinogen isoform, which has a unique N-terminal sequence, LPLDD (Fig. 1). The other three peaks proved to be trypsinogens but had the same N termini, FPVDD; therefore, these were subjected to in-gel tryptic digestion followed by mass spectrometric nanosequencing, which revealed the identity of the first peak as isoform T20 and the second and third peaks as isoforms T9 and T8 (Fig. 2A). The

latter two isoforms are nearly identical in their amino acid sequence (99% identity, Fig. 1) and MS/MS peptide coverage did not include any regions that were distinctive. On the basis of a slight difference in their ionic character, T9 was assigned to the second peak and T8 to the third peak. N-terminal sequencing of the combined second/third peaks after activation of trypsinogen to trypsin indicated a mixture of Val/Ile amino acids at position 35 (IVGGYTCRENS(V/I)P), with a preponderance of Val, confirming that the smaller second peak is T9 (containing

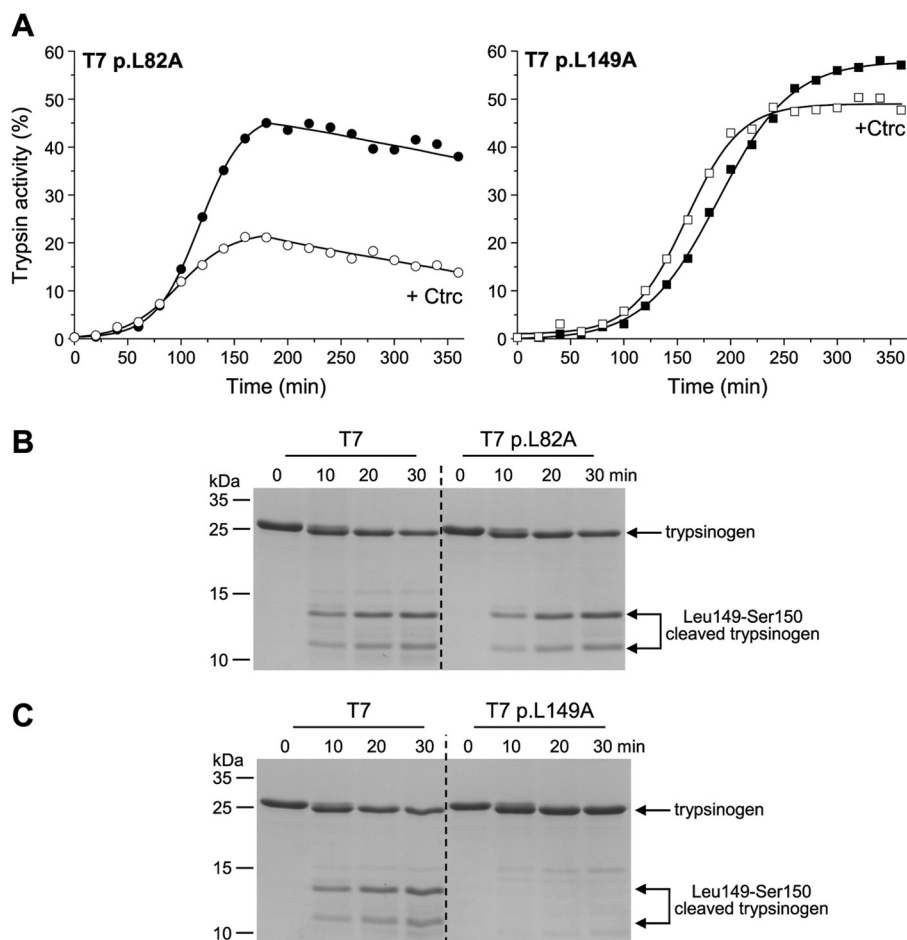


FIGURE 5. Effect of mutations p.L82A and p.L149A on mouse trypsinogen T7. *A*, autoactivation was measured in 1 mM CaCl_2 as described under "Experimental Procedures." Trypsin activity was expressed as percentage of the maximal activity determined by full activation with enteropeptidase. *B*, cleavage of wild-type and p.L82A T7 trypsinogen by 25 nM mouse Ctrc. *C*, cleavage of wild-type and p.L149A T7 trypsinogen by 25 nM mouse Ctrc. Incubations were performed with 2 μM trypsinogen in 0.1 M Tris-HCl (pH 8.0) in the absence of calcium. Trypsinogen samples were precipitated with trichloroacetic acid and analyzed by SDS-PAGE and Coomassie Blue staining. Representative experiments from two replicates are shown.

Ile-35) and the larger third peak is T8 (containing Val-35) (see Fig. 1). Both N-terminal sequencing (CGVPA) and MS/MS indicated that the T9/T8 peaks were contaminated with some Ctrb. Quantitative evaluation of trypsinogen peaks was performed as described under "Experimental Procedures," and the following relative expression levels were obtained (mean \pm S.D., $n = 4$): 41 \pm 1% for T7; 47 \pm 3% for T8 and T9 combined, and 12 \pm 2% for T20 (Table 2).

To confirm our findings with an independent method and in a different mouse strain, we used a proteomic approach based on two-dimensional PAGE, followed by in gel-digestion of silver-stained protein spots and peptide mass fingerprinting after MALDI-TOF mass spectrometry. Fig. 2*B* demonstrates two-dimensional PAGE protein patterns of a granule-enriched pancreas homogenate from the outbred NMRI mouse strain. In the 20–37-kDa molecular mass range, the same four trypsinogen isoforms were identified as with the chromatographic approach. The relative proportions of spot intensities (mean \pm S.D., $n = 4$) were 25 \pm 1% for T7, 33 \pm 1% for T8, 27 \pm 1% for T9, and 15 \pm 2% for T20 (Table 2). These values compare fairly well, within experimental error, with those obtained for CD-1 mice.

Autoactivation of Mouse Trypsinogens—Large scale purification of different trypsinogen isoforms from the mouse pancreas is impractical, and preparations may be contaminated with low levels of other pancreatic proteases. In contrast, recombinant expression should provide highly purified homogeneous enzyme preparations. We previously established methodology for the expression and purification of human trypsinogens (15, 16), and here we used the same approach to obtain functionally competent mouse trypsinogen preparations. Trypsinogens were expressed in *E. coli* as inclusion bodies, renatured *in vitro* and purified by ecotin-affinity chromatography. When mouse trypsinogens were incubated in 1 mM CaCl_2 at pH 8.0, isoforms T7, T8, and T9 autoactivated and reached about 40–60% of potentially attainable trypsin levels, indicating that some autocatalytic (trypsin-mediated) degradation occurred (Fig. 3*A*) during autoactivation. In contrast, T20 did not autoactivate under these conditions. As expected, high concentrations of calcium (10 mM) increased the rate of autoactivation and stabilized trypsinogens against degradation, yielding 80–100% of attainable trypsin levels. The stimulatory effect of calcium on the autoactivation of T20 was particularly striking (Fig. 3*B*).

Mouse Trypsinogens

Effect of Mouse Ctrc on T7 Trypsinogen—Addition of 25 nM mouse Ctrc to the autoactivation assays of isoform T7 moderately (by ~35%) reduced trypsin levels in 1 mM calcium and slightly stimulated the rate of autoactivation in 10 mM calcium (Fig. 4A). SDS-PAGE analysis of the autoactivation reaction in 1 mM calcium, in the absence of Ctrc, confirmed conversion of the T7 trypsinogen band to trypsin and also indicated degradation fragments generated by cleavages of trypsin-sensitive peptide bonds Arg-123–Val-124 and Lys-194–Asp-195 (Fig. 4B, left panel, see also Fig. 1). These were identified by N-terminal sequencing, similarity to the published degradation fragments of rat anionic trypsinogen-2 (26), and comparison of the banding pattern with that of the T7 p.R123H mutant (see below). Note that because of an extra amino acid in the activation peptide of T7, amino acid numbering is shifted by one relative to human and other mouse trypsinogens (see Fig. 1). Cleavage after Arg-123 should result in a fully active two-chain trypsin (27, 28), whereas cleavage after Lys-194 causes inactivation (26, 29). Ctrc caused a small shift of the T7 trypsinogen band, suggesting cleavage of the activation peptide (Fig. 4B, right panel). In addition, the banding pattern of degradation fragments became more complex, which is consistent with the lower trypsin activity attained during autoactivation in 1 mM calcium in the presence of Ctrc.

To identify Ctrc-mediated cleavages of trypsinogen, we performed digestion experiments with short incubation times when no trypsinogen activation took place and no trypsin activity was present. Under these conditions, slow cleavage of the Leu-149–Ser-150 peptide bond in the autolysis loop was observed in the absence of calcium (Fig. 4C, left panel), and this was completely inhibited by 10 mM calcium (Fig. 4C, right panel, see also Fig. 1). The Leu-82–Glu-83 peptide bond (corresponding to Leu-81–Glu-82 in human trypsinogens and other studied mouse isoforms) in the calcium binding loop was not cleaved to a detectable extent. This finding suggested that in T7 the moderate degradation observed during autoactivation in 1 mM calcium in the presence of Ctrc is mediated by cleavage of the Leu-149–Ser-150 peptide bond. To confirm this assumption, we compared autoactivation of the T7 p.L82A and p.L149A mutants in 1 mM calcium and found that only mutation of p.L149A protected against degradation in the presence of Ctrc (Fig. 5). Interestingly, mutant p.L82A suffered Ctrc-dependent degradation during autoactivation to an even larger extent than wild-type T7.

N-terminal Processing of T7 Trypsinogen by Mouse Ctrc—Among the activation peptide sequences of mouse trypsinogens, only T7 contains a potentially Ctrc-sensitive peptide bond, Leu-18–Asp-19 (Fig. 1). Inspection of Fig. 4B revealed that the T7 trypsinogen band became slightly shifted as a result of treatment with Ctrc, suggesting that the activation peptide might be cleaved at Leu-18–Asp-19. When samples were run under nonreducing conditions, the mobility shift caused by N-terminal processing of the T7 activation peptide became more apparent (Fig. 4D), and N-terminal sequencing confirmed the predicted cleavage site. However, in contrast to human cationic trypsinogen, the rate of autoactivation of N-terminally processed T7 was only negligibly stimulated (see Fig. 4A, right

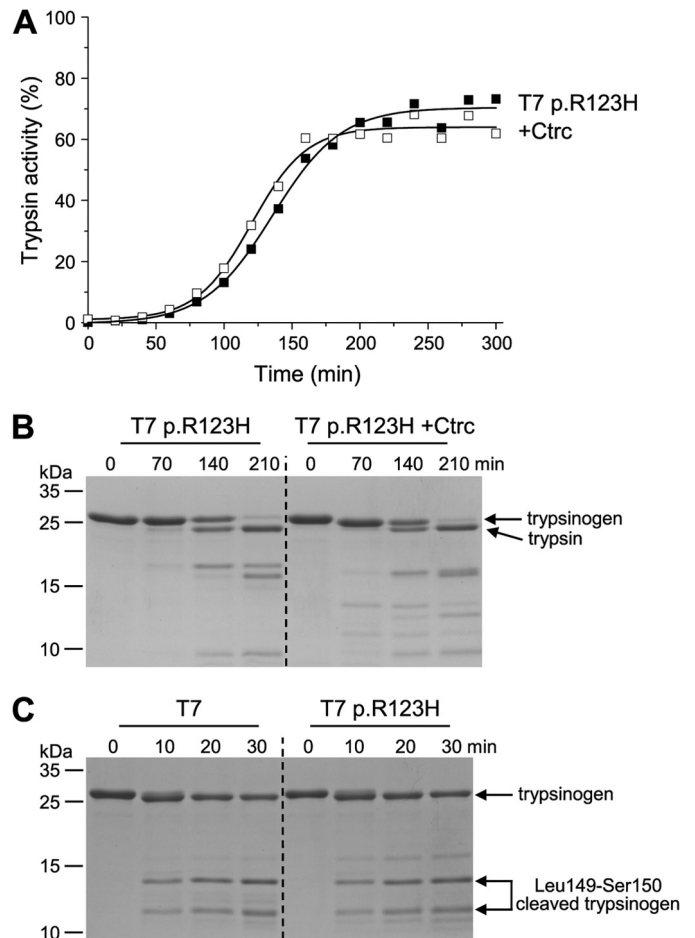


FIGURE 6. Effect of mutation p.R123H on mouse trypsinogen T7. A, autoactivation was measured in 1 mM CaCl₂ as described under "Experimental Procedures." Trypsin activity was expressed as percentage of the maximal activity determined by full activation with enteropeptidase. B, SDS-PAGE analysis of the autoactivation reaction. Samples were withdrawn at indicated times, precipitated with trichloroacetic acid, electrophoresed, and stained as described under "Experimental Procedures." C, cleavage of wild-type and p.R123H T7 trypsinogen by 25 nM mouse Ctrc. Incubations were performed with 2 μM trypsinogen in 0.1 M Tris-HCl (pH 8.0) in the absence of calcium. Samples were precipitated with trichloroacetic acid and analyzed by SDS-PAGE and Coomassie Blue staining. Cleavage products were identified with N-terminal sequencing. Representative experiments from two replicates are shown.

panel), indicating that Ctrc does not regulate activation of mouse trypsinogens through cleavage of the activation peptide.

Effect of the p.R123H Mutation on T7 Trypsinogen—Mutation p.R123H protected T7 trypsinogen against degradation during autoactivation in 1 mM calcium in the presence of Ctrc (Fig. 6); however, it had no effect on the cleavage of the Leu-149–Ser-150 peptide bond *per se*. This observation indicates that moderate degradation of T7 during autoactivation is due to the combined effects of Ctrc-mediated and tryptic cleavages after Leu-149 and Arg-123, respectively (see Fig. 1).

Effect of Mouse Ctrc on T8 and T9 Trypsinogen—Mouse Ctrc almost completely inhibited autoactivation of T8 and T9 trypsinogen in 1 mM calcium and markedly reduced it in 10 mM calcium (Figs. 7 and 8). This inhibitory effect was not due to degradation, as addition of enteropeptidase to the Ctrc-treated samples resulted in the appearance of highly significant trypsin activity. SDS-PAGE analysis of autoactivation in 1 mM calcium,

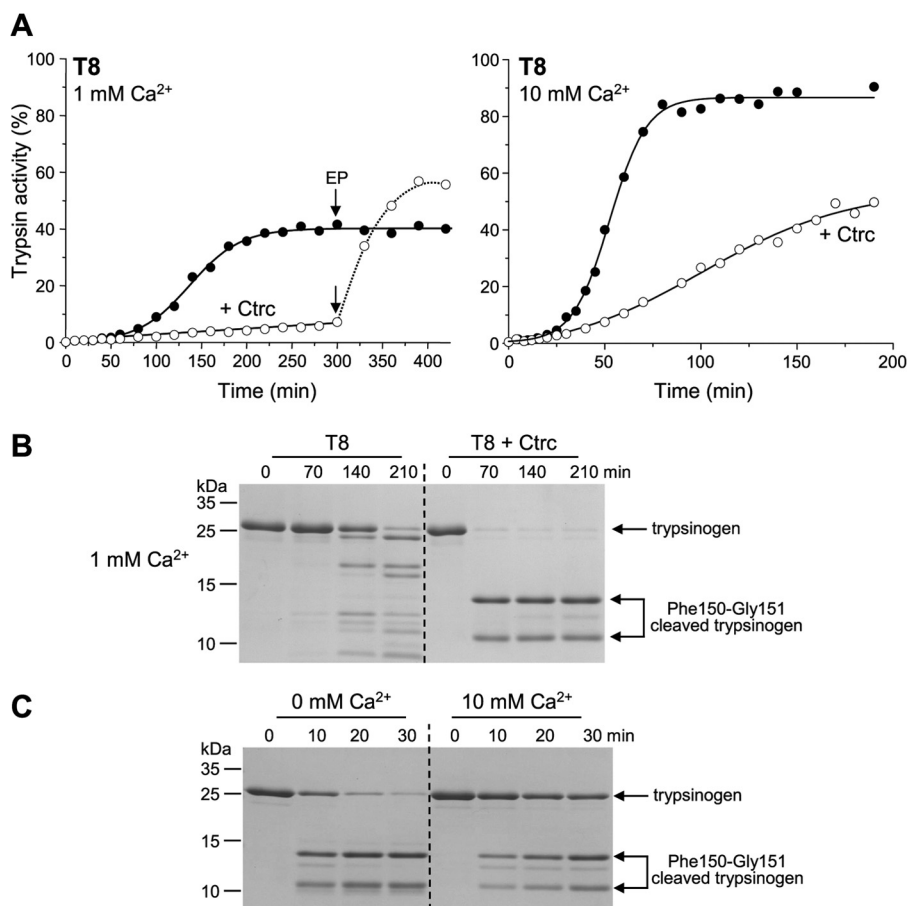


FIGURE 7. Effect of mouse Ctrc on mouse trypsinogen T8. *A*, autoactivation was measured in 1 and 10 mM CaCl₂, in the absence (solid symbols) or presence (open symbols) of 25 nM mouse Ctrc, as described under "Experimental Procedures." Where indicated, 2 μ l of 1.4 μ g/ml human enteropeptidase (EP) was added. *B*, SDS-PAGE analysis of the autoactivation reaction in 1 mM CaCl₂. Samples were withdrawn at indicated times, precipitated with trichloroacetic acid, electrophoresed, and stained as described under "Experimental Procedures." *C*, cleavage of trypsinogen by 25 nM mouse Ctrc. Incubations were performed with 2 μ M trypsinogen in 0.1 M Tris-HCl (pH 8.0) in the absence or presence of 10 mM CaCl₂. Samples were precipitated with trichloroacetic acid and analyzed by SDS-PAGE and Coomassie Blue staining. Cleavage products were identified with N-terminal sequencing. In the absence of calcium (left panel), the faint bands above and below the major cleavage products correspond to fragments of trypsinogen cleaved at the Leu-81–Glu-82 peptide bond. The faint band visible in the presence of 10 mM calcium (right panel) could not be identified. Representative experiments from three replicates are shown.

in the absence of Ctrc, demonstrated conversion of trypsinogen to trypsin with the characteristic degradation fragments generated by tryptic cleavage of the Arg-122–Val-123 and Lys-193–Asp-194 peptide bonds (Figs. 7*B* and 8*B*, left panel, see also Fig. 1). In dramatic contrast, when autoactivation was followed in the presence of Ctrc, no trypsin band nor any of the tryptic degradation bands were observed. Instead, Ctrc rapidly and completely cleaved T8 and T9 trypsinogen at a single site, which N-terminal sequencing revealed as the Phe-150–Gly-151 peptide bond (Figs. 7*B* and 8*B*, right panel). This peptide bond lies within the so-called autolysis loop, a flexible segment between residues 146 and 154 (Fig. 1). When cleavage of T8 and T9 trypsinogen by Ctrc was studied with short incubation times (*i.e.* before autoactivation occurred), both isoforms were primarily cleaved at the Phe-150–Gly-151 peptide bond, with minimal cleavage observed at the Leu-81–Glu-82 peptide bond in the absence of calcium (Figs. 7*C* and 8*C*). Cleavage of the Phe-150–Gly-151 peptide bond was slower but still readily detectable in 10 mM calcium.

Cleavage of the Phe-150–Gly-151 Peptide Bond by Mouse Chymotrypsin B (Ctrb)—Regulation of autoactivation of human cationic trypsinogen by human CTRC is highly specific, and

other chymotrypsins and elastases do not cleave the CTRC cleavage sites. To test whether the same Ctrc specificity exists in the mouse, we compared the effect of mouse Ctrb and Ctrc on T8 trypsinogen. As shown in Fig. 9*A*, autoactivation of T8 was much less effectively inhibited by 25 nM Ctrb than by an equimolar concentration of Ctrc. In degradation experiments, Ctrb cleaved the Phe-150–Gly-151 peptide bond at a more than 7-fold slower rate than Ctrc (Fig. 9, *B* and *C*).

Effect of the p.R122H Mutation on T8 Trypsinogen—Mutation p.R122H slightly stimulated autoactivation of T8 trypsinogen in 1 mM calcium, in the absence of Ctrc (Fig. 10*A*). In the presence of Ctrc, however, autoactivation was strongly inhibited by Ctrc, approximately to the same extent as seen with wild-type T8 (Fig. 10*B*, *cf.* Fig. 7*A*). Consistent with the robust inhibitory effect, the Phe-150–Gly-151 peptide bond was cleaved by Ctrc almost as well in T8 p.R122H trypsinogen as in wild-type T8 (Fig. 10*C*).

Cleavage of the Autolysis Loop in the p.S150F Human Cationic Trypsinogen Mutant Inhibits Autoactivation—The majority of mammalian trypsinogens do not contain Phe-150 in their autolysis loop. To test whether introduction of Phe-150 would reconstitute the chymotrypsin-dependent autoactivation inhi-

Mouse Trypsinogens

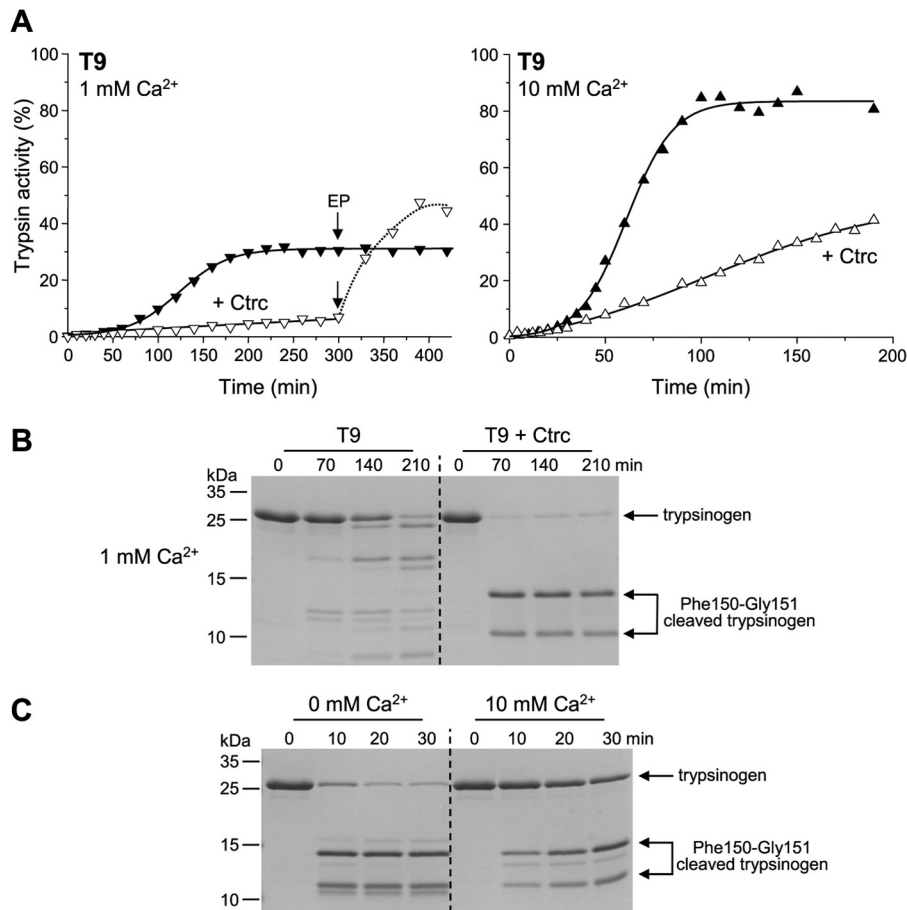


FIGURE 8. Effect of mouse Ctrc on mouse trypsinogen T9. See Fig. 7 for experimental details. EP, human enteropeptidase.

bition in another mammalian trypsinogen, we mutated Ser-150 in human cationic trypsinogen to Phe. Because human CTRC cleaves the Leu-81–Glu-82 peptide bond and causes trypsinogen degradation, we used human CTRB2 to selectively cleave the newly created Phe-150–Gly-151 peptide bond. CTRB2 at 25 nM concentration had no effect on the autoactivation of wild-type cationic trypsinogen (Fig. 11A), but it inhibited activation of the p.S150F mutant (Fig. 11B), via cleavage at the Phe-150–Gly-151 peptide bond (Fig. 11C).

Effect of Mouse Ctrc on T20 Trypsinogen—Finally, mouse Ctrc had essentially no effect on trypsinogen T20, except for a slight stimulation of the activation rate in 10 mM calcium (Fig. 12A). On SDS-PAGE, no trypsinogen to trypsin conversion was evident in 1 mM calcium, in the absence or presence of Ctrc (Fig. 12B). Note that T20 trypsinogen ran as a doublet on gels, which seems to represent differently denatured conformers, as N-terminal sequencing and mass spectrometry indicated molecular homogeneity (data not shown). Finally, cleavage of T20 with Ctrc resulted in very faint degradation bands even in the absence of calcium, indicating that this isoform is resistant to Ctrc (Fig. 12C).

DISCUSSION

The aim of this study was to identify the major trypsinogen isoforms expressed by the mouse pancreas and characterize their regulation of autoactivation by mouse Ctrc. These studies were undertaken to clarify whether introduction of trypsinogen

mutations associated with human hereditary pancreatitis into mouse trypsinogens would offer a viable approach to model hereditary pancreatitis in mice. Previous attempts to generate transgenic mice expressing the coding DNA for human cationic trypsinogen with the p.R122H mutation failed to recapitulate hereditary pancreatitis, partly because of the low transgene expression levels (6). Introduction of mutation p.R122H into an endogenous mouse trypsinogen may circumvent the expression problem. However, the effect of p.R122H in human cationic trypsinogen is dependent on CTRC (3), and it has been unknown whether autoactivation of mouse trypsinogens is regulated by mouse Ctrc in a manner that mimics the human situation.

Using two independent biochemical approaches with two commonly used outbred mouse strains, we found that only four trypsinogen isoforms, T7, T8, T9 and T20, are expressed to high levels (Table 2) in the mouse pancreas, even though the mouse genome contains 20 trypsinogen genes, of which 11 are potentially functional (Table 1 and Fig. 1). The cationic isoform T7 was recently deleted in the C57BL/6 strain, and judging from the residual trypsinogen content the authors suggested that T7 contributes 60% of total mouse trypsinogens (12, 13). Here, we obtained smaller values (41% in CD-1 and 25% in NMRI mice); however, these differences seem to fall within experimental error and may even represent strain-specific differences. It is important to note that Prss1 (T16) and Prss3 (T11) (see Table

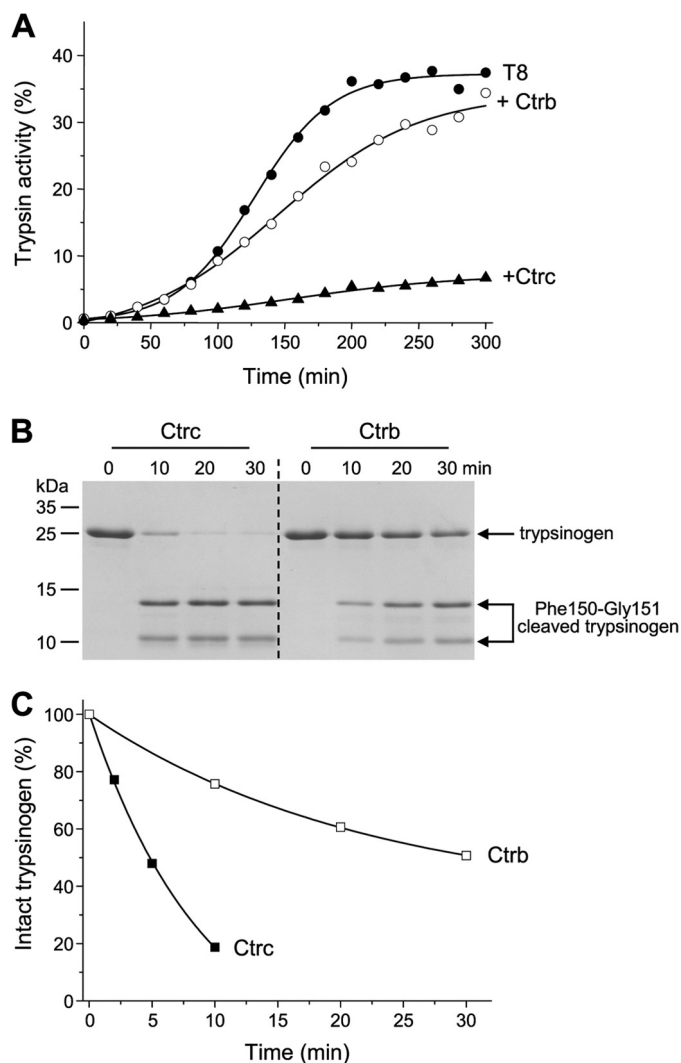


FIGURE 9. Effect of mouse Ctrb on mouse trypsinogen T8. *A*, autoactivation was measured in 1 mM CaCl₂ as described under "Experimental Procedures" in the absence or presence of 25 nM mouse Ctrb or Ctrc, as indicated. *B*, cleavage of trypsinogen by 25 nM Ctrb and Ctrc was compared in the absence of calcium, as described in Fig. 7C. Representative experiments from two replicates are shown. *C*, disappearance of the intact trypsinogen band was quantitated by densitometry, and data from two experiments were plotted. For clarity, error bars were omitted; the error was within 10% of the mean.

1), the presumed orthologs of human cationic trypsinogen (PRSS1) and mesotrypsinogen (PRSS3), are not expressed at detectable levels, indicating that assignment of orthology by database curators may be unreliable and even misleading to investigators, as evidenced by a recent study where expression of mouse Prss1 was studied (30). Finally, we emphasize that our data pertain to the resting, unstimulated mouse pancreas, and it is possible, even likely, that upon hormonal stimulation the trypsinogen expression pattern may change, as shown previously for rat p23, the ortholog of mouse T4 and T5, which becomes drastically up-regulated upon cerulein stimulation (31). Marked up-regulation of T5 was observed in a knock-out mouse strain deficient in interferon regulatory factor 2 (32).

Autoactivation of mouse trypsinogens T7, T8, and T9 was comparable, whereas T20 autoactivated more slowly, particularly in 1 mM calcium (see Fig. 3). Surprisingly, regulation of autoactivation by mouse Ctrc was isoform-specific and mech-

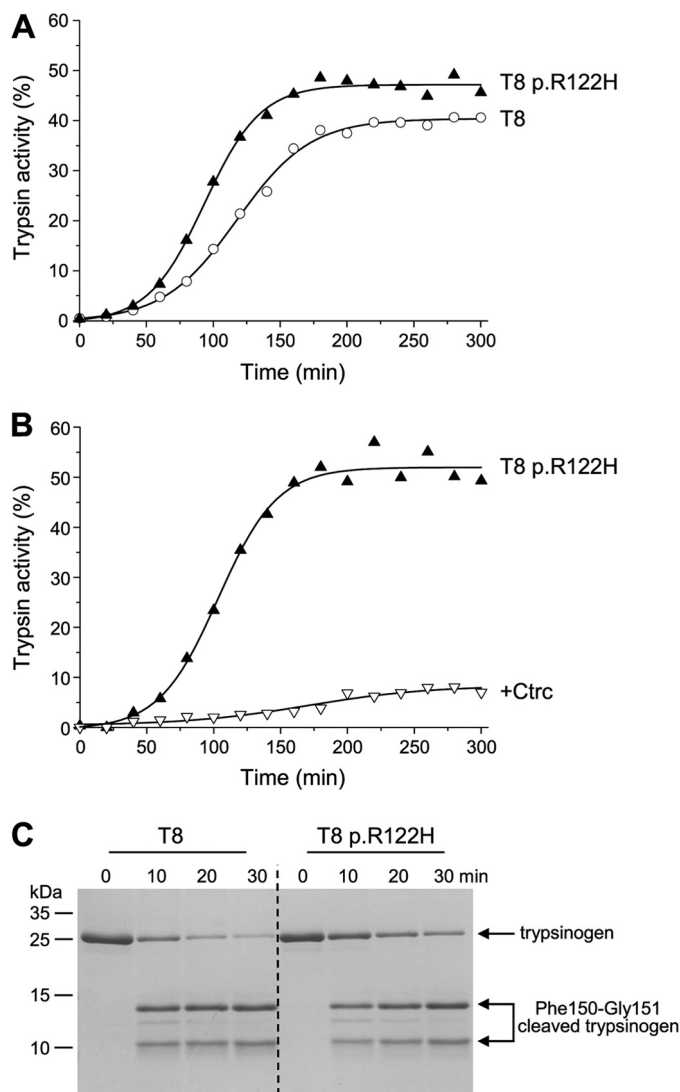


FIGURE 10. Effect of mutation p.R122H on mouse trypsinogen T8. *A*, autoactivation of wild-type and p.R122H mutant T8 trypsinogen was measured in 1 mM CaCl₂ as described under "Experimental Procedures." *B*, effect of 25 nM mouse Ctrc on the autoactivation of the p.R122H mutant T8. Conditions were the same as in *A*. *C*, cleavage of wild-type and p.R122H mutant T8 trypsinogen by 25 nM mouse Ctrc in the absence of calcium. Samples were incubated and analyzed as described in Fig. 7C. Representative experiments from two replicates are shown.

anistically different from the actions of human CTRC on human cationic trypsinogen. Whereas the human enzyme targets regulatory cleavage sites in the activation peptide and the calcium binding loop of cationic trypsinogen, these proved to be irrelevant in mouse trypsinogens. Thus, Ctrc-mediated cleavage of the activation peptide was observed only with the T7 isoform, however, this N-terminal processing had no significant effect on autoactivation. Cleavage of the Leu-81–Glu-82 peptide bond in the calcium binding loop (Leu-82–Glu-83 in T7) was not detectable in T7 or T20, and minimal cleavage was seen in T8 and T9. In contrast, isoforms T8 and T9 were rapidly cleaved at the Phe-150–Gly-151 peptide bond in the autolysis loop, and this cleavage resulted in marked inhibition of autoactivation. The Phe-150–Gly-151 peptide bond was also cleaved by Ctrb at a 7-fold slower rate. However, considering that Ctrb is the most abundant chymotrypsin in the pancreas, physiolog-

Mouse Trypsinogens

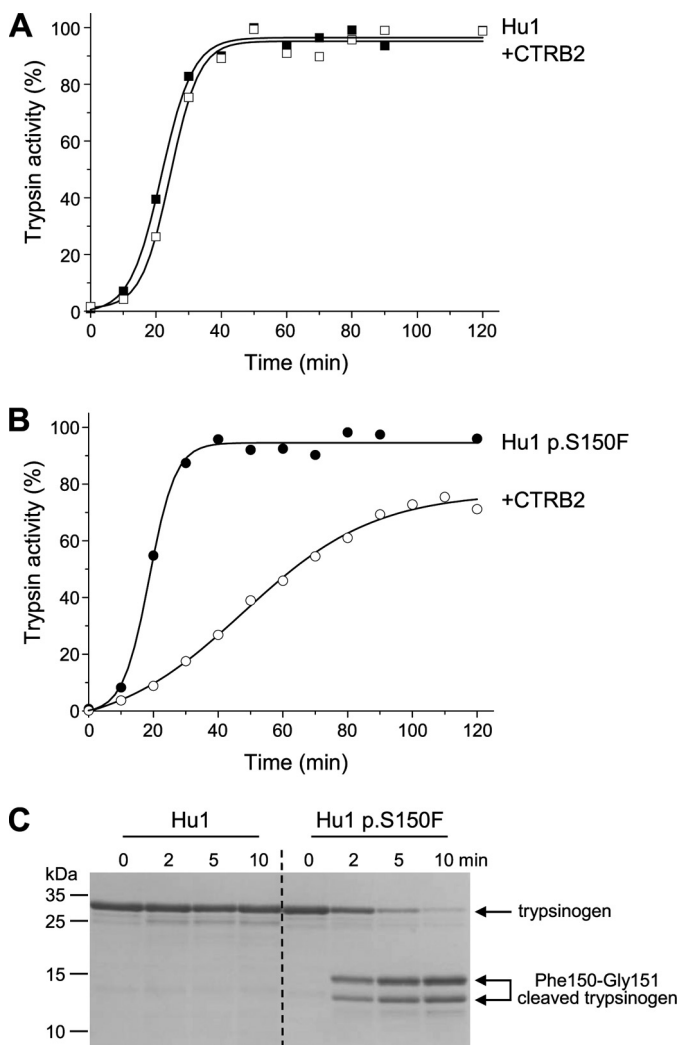


FIGURE 11. Effect of human CTRB2 on the autoactivation of wild-type and p.S150F mutant human cationic trypsinogen (Hu1). *A* and *B*, autoactivation was measured in 1 mM CaCl₂ in the absence or presence of 25 nM CTRB2, as described under "Experimental Procedures." *C*, cleavage of wild-type and p.S150F mutant human cationic trypsinogen by 25 nM CTRB2 in the absence of calcium. Incubations were performed, and samples were analyzed as given in Fig. 7C. To prevent autoactivation, 25 nM human SPINK1 trypsin inhibitor was included. Representative experiments from two replicates are shown.

ical regulation of activation of T8 and T9 may be also dependent on Ctrb. Isoform T7 was also cleaved in the autolysis loop, albeit slowly and at a different peptide bond (Leu-149–Ser-150), which resulted in moderate degradation during autoactivation. Nevertheless, isoform T7 was clearly less sensitive to chymotryptic regulation than human cationic trypsinogen or mouse trypsinogens T8 and T9.

The lack of cleavage at the Leu-81–Glu-82 (Leu-82–Glu-83 in T7) peptide bond by Ctrc may be partly explained by differences in the amino acid sequence of the calcium binding loop (see Fig. 1). Furthermore, as we learned from the recent crystal structure of human CTRC, recognition of the calcium binding loop is governed by long range electrostatic interactions between the negatively charged substrate and positively charged surface regions on CTRC (33). These macroscopic electrostatic interactions are less favorable in the mouse, due to missing positively charged residues in Ctrc (Arg-80 and Arg-

240) and negatively charged residues in mouse trypsinogens T7 (Glu-32, Asp-156, and Glu-157) and T8, T9, and T20 (Glu-79 and Glu-157) (see Fig. 1).

The majority of mammalian trypsinogens do not contain Phe-150, indicating that this novel mechanism of autoactivation regulation may be unique to rodents. Human mesotrypsinogen contains Phe-150, and cleavage at this site by human CTRC was demonstrated previously (5), suggesting that activation of mesotrypsinogen may be under similar regulation. Human anionic and cationic trypsinogens contain Ser at position 150, but mutation S150F confers sensitivity to CTRB2-mediated cleavage of the autolysis loop, which inhibits autoactivation in a manner that is similar to the Ctrc-dependent inhibition of T8 and T9 in the mouse. Crystal structures of mouse trypsinogens are not available, and the autolysis loop in structures of rat anionic trypsinogen is disordered and not visible. Therefore, we used a bovine trypsinogen structure to model the potential effects of cleavage of the autolysis loop after Phe-150. As shown in Fig. 13, the autolysis loop may be in close proximity to the trypsinogen activation peptide, at least judged by the position of Val-25, the first visible residue of the otherwise disordered N-terminal segment. Cleavage of the Phe-150–Gly-151 peptide bond should increase the mobility of the autolysis loop, which may directly interact with the activation peptide thereby decreasing its accessibility. One possible interaction may occur between the positive charge of the newly created N terminus in the autolysis loop and the negatively charged tetra-Asp motif in the activation peptide.

The Ctrc-dependent inhibition of autoactivation of T8 and T9 trypsinogens may have evolved as a protective mechanism to curtail unwanted trypsinogen activation in the pancreas. This is conceptually analogous to the regulation of human trypsinogens by human CTRC even though mechanistic details are dissimilar. Interestingly, we found that cleavage of the Phe-150–Gly-151 peptide bond in T8 and T9 trypsinogens also inhibits activation by enteropeptidase, the physiological trypsinogen activator in the duodenum (data not shown). Although inhibition of digestive enzyme activation in the gut may seem counterintuitive, this chymotrypsin-dependent feedback mechanism likely ensures that intestinal trypsinogen activation proceeds with a slower, more prolonged kinetics, which may be favorable for food digestion.

Intra-acinar cell activation of trypsinogen in cytoplasmic vesicles of autophagic origin is an early event in experimental models of acute pancreatitis (34). Genetic deletion of T7 was recently shown to abolish intra-acinar trypsinogen activation in response to hyperstimulation with cerulein: a somewhat perplexing observation as other trypsinogen isoforms could have potentially be activated (12, 13). The results presented here offer a plausible explanation for this puzzle. When trypsinogen activation occurs, isoforms T8 and T9 may be inhibited in a Ctrc or Ctrb-dependent manner, whereas T7 is less sensitive to chymotryptic regulation. Because of its lower concentration and poor activation, isoform T20 is unlikely to contribute to intra-acinar trypsinogen activation to a detectable extent.

Finally, our data argue that in the context of mouse trypsinogens, human pancreatitis-associated mutations may not recapitulate the pathogenic biochemical phenotype observed with

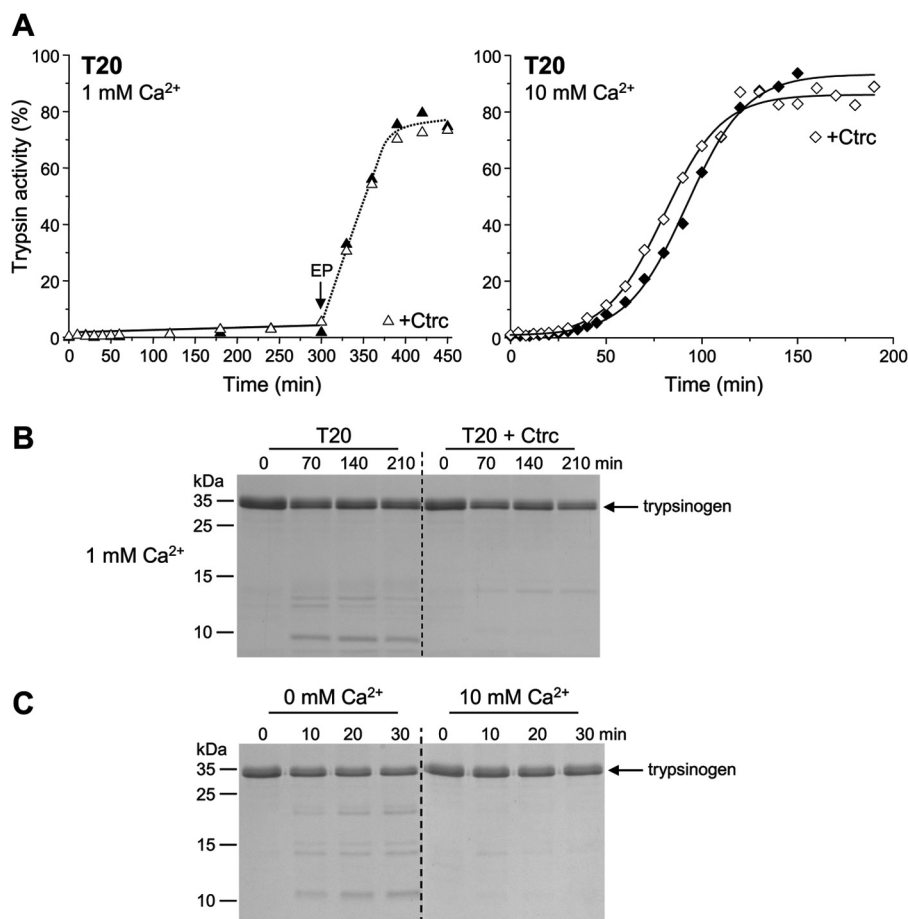


FIGURE 12. **Effect of mouse Ctrc on mouse trypsinogen T20.** *A*, autoactivation was measured in 1 and 10 mM CaCl₂ in the absence (*solid symbols*) or presence (*open symbols*) of 25 nM mouse Ctrc, as described under "Experimental Procedures." Where indicated, 2 μl of 1.4 μg/ml human enteropeptidase (EP) was added. *B*, SDS-PAGE analysis of the autoactivation reaction in 1 mM CaCl₂. Samples were withdrawn at the indicated time points, precipitated with trichloroacetic acid, electrophoresed, and stained as described under "Experimental Procedures." *C*, cleavage of T20 trypsinogen by 25 nM mouse Ctrc. Incubations were performed, and samples were analyzed as in Fig. 7C. The faint Ctrc cleavage products seen in the absence of calcium were not identified. Representative experiments from three replicates are shown.

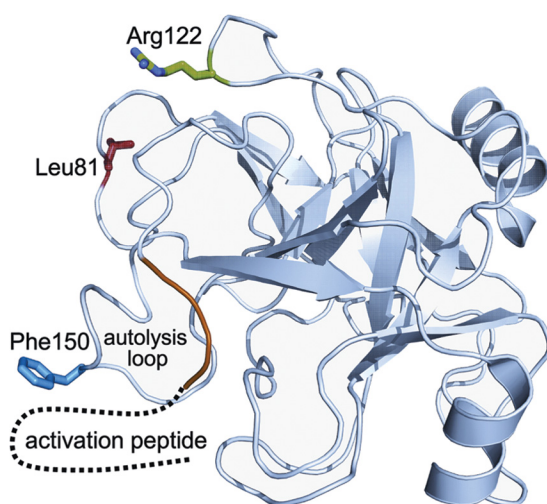


FIGURE 13. **Proximity of the autolysis loop and the activation peptide in trypsinogen.** Mouse trypsinogen T8 was modeled using a ribbon diagram of bovine trypsinogen (Protein Data Bank code 1TGN). The side chains for amino acids Leu-81, Arg-122, and Phe-150 are indicated. The putative activation peptide backbone is indicated by *dotted lines*. In the crystal structure the activation peptide (residues 16–23) is disordered, and the first visible N-terminal amino acid is valine 25. The image was rendered using PyMOL 1.3 (Schrodinger, LLC).

human cationic trypsinogen. We found that mutation p.R122H did not affect inhibition of autoactivation by Ctrc in T8 trypsinogen, which stands in contrast to the robust negative effect of this mutation on CTRC-dependent degradation of human cationic trypsinogen (3). Thus, introduction of human mutations into mouse trypsinogens may not be a practical approach for the generation of mouse models of human hereditary pancreatitis.

Acknowledgments—András Szabó is gratefully acknowledged for help with structural modeling and experimental advice. We thank Sebastian Beer for help with mutagenesis.

REFERENCES

- Whitcomb, D. C., Gorry, M. C., Preston, R. A., Furey, W., Sossenheimer, M. J., Ulrich, C. D., Martin, S. P., Gates, L. K., Jr., Amann, S. T., Toskes, P. P., Liddle, R., McGrath, K., Uomo, G., Post, J. C., and Ehrlich, G. D. (1996) Hereditary pancreatitis is caused by a mutation in the cationic trypsinogen gene. *Nat. Genet.* **14**, 141–145
- Teich, N., Rosendahl, J., Tóth, M., Mössner, J., and Sahin-Tóth, M. (2006) Mutations of human cationic trypsinogen (PRSS1) and chronic pancreatitis. *Hum. Mutat.* **27**, 721–730
- Szabó, A., and Sahin-Tóth, M. (2012) Increased activation of hereditary pancreatitis-associated human cationic trypsinogen mutants in presence

- of chymotrypsin *C. J. Biol. Chem.* **287**, 20701–20710
4. Nemoda, Z., and Sahin-Tóth, M. (2006) Chymotrypsin C (caldecrin) stimulates autoactivation of human cationic trypsinogen. *J. Biol. Chem.* **281**, 11879–11886
 5. Szmola, R., and Sahin-Tóth, M. (2007) Chymotrypsin C (caldecrin) promotes degradation of human cationic trypsin: identity with Rinderknecht's enzyme *Y. Proc. Natl. Acad. Sci. U.S.A.* **104**, 11227–11232
 6. Selig, L., Sack, U., Gaiser, S., Klöppel, G., Savkovic, V., Mössner, J., Keim, V., and Bödeker, H. (2006) Characterisation of a transgenic mouse expressing R122H human cationic trypsinogen. *BMC Gastroenterol.* **6**, 30
 7. Archer, H., Jura, N., Keller, J., Jacobson, M., and Bar-Sagi, D. (2006) A mouse model of hereditary pancreatitis generated by transgenic expression of R122H trypsinogen. *Gastroenterology* **131**, 1844–1855
 8. Watanabe, T., and Ogasawara, N. (1982) Purification and properties of multiple forms of mouse trypsinogen. *Biochim. Biophys. Acta* **717**, 439–444
 9. Stevenson, B. J., Hagenbüchle, O., and Wellauer, P. K. (1986) Sequence organisation and transcriptional regulation of the mouse elastase II and trypsin genes. *Nucleic Acids Res.* **14**, 8307–8330
 10. Glusman, G., Rowen, L., Lee, I., Boysen, C., Roach, J. C., Smit, A. F., Wang, K., Koop, B. F., and Hood, L. (2001) Comparative genomics of the human and mouse T cell receptor loci. *Immunity* **15**, 337–349
 11. Ohmura, K., Kohno, N., Kobayashi, Y., Yamagata, K., Sato, S., Kashiwabara, S., and Baba, T. (1999) A homologue of pancreatic trypsin is localized in the acrosome of mammalian sperm and is released during acrosome reaction. *J. Biol. Chem.* **274**, 29426–29432
 12. Dawra, R., Sah, R. P., Dudeja, V., Rishi, L., Talukdar, R., Garg, P., and Saluja, A. K. (2011) Intra-acinar trypsinogen activation mediates early stages of pancreatic injury but not inflammation in mice with acute pancreatitis. *Gastroenterology* **141**, 2210–2217
 13. Sah, R. P., Dudeja, V., Dawra, R. K., and Saluja, A. K. (2013) Caerulein-induced chronic pancreatitis does not require intra-acinar activation of trypsinogen in mice. *Gastroenterology* **144**, 1076–1085
 14. Király, O., Guan, L., Szepessy, E., Tóth, M., Kukor, Z., and Sahin-Tóth, M. (2006) Expression of human cationic trypsinogen with an authentic N terminus using intein-mediated splicing in aminopeptidase P-deficient *Escherichia coli*. *Protein Expr. Purif.* **48**, 104–111
 15. Sahin-Tóth, M. (2000) Human cationic trypsinogen. Role of Asn-21 in zymogen activation and implications in hereditary pancreatitis. *J. Biol. Chem.* **275**, 22750–22755
 16. Sahin-Tóth, M., and Tóth, M. (2000) Gain-of-function mutations associated with hereditary pancreatitis enhance autoactivation of human cationic trypsinogen. *Biochem. Biophys. Res. Commun.* **278**, 286–289
 17. Pál, G., Sprengel, G., Patthy, A., and Gráf, L. (1994) Alteration of the specificity of ecotin, an *E. coli* serine proteinase inhibitor, by site-directed mutagenesis. *FEBS Lett.* **342**, 57–60
 18. Lengyel, Z., Pál, G., and Sahin-Tóth, M. (1998) Affinity purification of recombinant trypsinogen using immobilized ecotin. *Protein Expr. Purif.* **12**, 291–294
 19. Schagger, H., and von Jagow, G. (1987) Tricine-sodium dodecyl sulfate-polyacrylamide gel electrophoresis for the separation of proteins in the range from 1 to 100 kDa. *Anal. Biochem.* **166**, 368–379
 20. Blum, H., Beier, H., and Gross, H. J. (1987) Improved silver staining of plant proteins, RNA and DNA in polyacrylamide gels. *Electrophoresis* **8**, 93–99
 21. Neuhoff, V., Arold, N., Taube, D., and Ehrhardt, W. (1988) Improved staining of proteins in polyacrylamide gels including isoelectric focusing gels with clear background at nanogram sensitivity using Coomassie Brilliant Blue G-250 and R-250. *Electrophoresis* **9**, 255–262
 22. Király, O., Guan, L., and Sahin-Tóth, M. (2011) Expression of recombinant proteins with uniform N termini. *Methods Mol. Biol.* **705**, 175–194
 23. Szabó, A., and Sahin-Tóth, M. (2012) Determinants of chymotrypsin C cleavage specificity in the calcium-binding loop of human cationic trypsinogen. *FEBS J.* **279**, 4283–4292
 24. Szabó, A., Héja, D., Szakács, D., Zboray, K., Kékesi, K. A., Radisky, E. S., Sahin-Tóth, M., and Pál, G. (2011) High affinity small protein inhibitors of human chymotrypsin C (CTRC) selected by phage display reveal unusual preference for P4' acidic residues. *J. Biol. Chem.* **286**, 22535–22545
 25. Kukor, Z., Tóth, M., and Sahin-Tóth, M. (2003) Human anionic trypsinogen: properties of autocatalytic activation and degradation and implications in pancreatic diseases. *Eur. J. Biochem.* **270**, 2047–2058
 26. Sahin-Tóth, M. (1999) Hereditary pancreatitis-associated mutation Asn²¹ → Ile stabilizes rat trypsinogen *in vitro*. *J. Biol. Chem.* **274**, 29699–29704
 27. Maroux, S., and Desnuelle, P. (1969) On some autolyzed derivatives of bovine trypsin. *Biochim. Biophys. Acta* **181**, 59–72
 28. Kukor, Z., Tóth, M., Pál, G., and Sahin-Tóth, M. (2002) Human cationic trypsinogen. Arg-117 is the reactive site of an inhibitory surface loop that controls spontaneous zymogen activation. *J. Biol. Chem.* **277**, 6111–6117
 29. Smith, R. L., and Shaw, E. (1969) Pseudotrypsin. A modified bovine trypsin produced by limited autodigestion. *J. Biol. Chem.* **244**, 4704–4712
 30. Wang, J., Ohmuraya, M., Suyama, K., Hirota, M., Ozaki, N., Baba, H., Nakagata, N., Araki, K., and Yamamura, K. (2010) Relationship of strain-dependent susceptibility to experimentally induced acute pancreatitis with regulation of Prss1 and Spink3 expression. *Lab. Invest.* **90**, 654–664
 31. Lütcke, H., Rausch, U., Vasiloudes, P., Scheele, G. A., and Kern, H. F. (1989) A fourth trypsinogen (P23) in the rat pancreas induced by CCK. *Nucleic Acids Res.* **17**, 6736
 32. Hayashi, H., Kohno, T., Yasui, K., Murota, H., Kimura, T., Duncan, G. S., Nakashima, T., Yamamoto, K., Katayama, I., Ma, Y., Chua, K. J., Suematsu, T., Shimokawa, I., Akira, S., Kubo, Y., Mak, T. W., and Matsuyama, T. (2011) Characterization of dsRNA-induced pancreatitis model reveals the regulatory role of IFN regulatory factor 2 (Irf2) in trypsinogen5 gene transcription. *Proc. Natl. Acad. Sci. U.S.A.* **108**, 18766–18771
 33. Batra, J., Szabó, A., Caulfield, T. R., Soares, A. S., Sahin-Tóth, M., and Radisky, E. S. (2013) Long-range electrostatic complementarity governs substrate recognition by human chymotrypsin C, a key regulator of digestive enzyme activation. *J. Biol. Chem.* **288**, 9848–9859
 34. Sah, R. P., Garg, P., and Saluja, A. K. (2012) Pathogenic mechanisms of acute pancreatitis. *Curr. Opin. Gastroenterol.* **28**, 507–515